RESEARCH ARTICLE

Regional Precuneus Cortical Hyperexcitability in Alzheimer's Disease Patients

Elias P. Casula, PhD [1,2] Ilaria Borghi, MSc,[1,3] Michele Maiella, MSc,[1]
Maria C. Pellicciari, PhD,[1] Sonia Bonnì, PhD,[1] Lucia Mencarelli, PhD,[1]
Martina Assogna, MD,[1] Alessia D'Acunto, BSc,[1] Francesco Di Lorenzo, MD,[1]
Danny A. Spampinato, PhD,[1] Emiliano Santarnecchi, PhD,[4]
Alessandro Martorana, MD, PhD,[5] and Giacomo Koch, MD, PhD [1,6]

Objective: Neuronal excitation/inhibition (E/I) imbalance is a potential cause of neuronal network malfunctioning in Alzheimer's disease (AD), contributing to cognitive dysfunction. Here, we used a novel approach combining transcranial magnetic stimulation (TMS) and electroencephalography (EEG) to probe cortical excitability in different brain areas known to be directly involved in AD pathology.
Methods: We performed TMS-EEG recordings targeting the left dorsolateral prefrontal cortex (l-DLPFC), the left posterior parietal cortex (l-PPC), and the precuneus (PC) in a large sample of patients with mild-to-moderate AD (n = 65) that were compared with a group of age-matched healthy controls (n = 21).
Results: We found that patients with AD are characterized by a regional cortical hyperexcitability in the PC and, to some extent, in the frontal lobe, as measured by TMS-evoked potentials. Notably, cortical excitability assessed over the l-PPC was comparable between the 2 groups. Furthermore, we found that the individual level of PC excitability was associated with the level of cognitive impairment, as measured with Mini-Mental State Examination, and with corticospinal fluid levels of $A\beta_{42}$.
Interpretation: Our data provide novel evidence that precuneus cortical hyperexcitability is a key feature of synaptic dysfunction in patients with AD. The current results point to the combined approach of TMS and EEG as a novel promising technique to measure hyperexcitability in patients with AD. This index could represent a useful biomarker to stage disease severity and evaluate response to novel therapies.

ANN NEUROL 2022;00:1–13

Abbreviations

Aβ	amyloid beta
AD	Alzheimer's disease
CDR	clinical dementia score
ChAT	choline acetyltransferase
CSF	cerebrospinal fluid
DLPFC	dorso-lateral prefrontal cortex
DMN	default mode network
E/I	excitation/inhibition
EEG	electroencephalography

View this article online at wileyonlinelibrary.com. DOI: 10.1002/ana.26514

Received Jun 10, 2022, and in revised form Sep 5, 2022. Accepted for publication Sep 12, 2022.

Address correspondence to Dr Koch, Experimental Neuropsychophysiology Lab, Department of Behavioral and Clinical Neurology, Santa Lucia Foundation IRCCS, Via Ardeatina, 306, 00179, Rome, Italy. E-mail: g.koch@hsantalucia.it

From the [1]Department of Behavioral and Clinical Neurology, Santa Lucia Foundation IRCCS, Rome, Italy; [2]Department of Psychology, La Sapienza University, Rome, Italy; [3]Center for Translational Neurophysiology of Speech and Communication (CTNSC), Italian Institute of Technology (IIT), Ferrara, Italy; [4]Gordon Center for Medical Imaging, Department of Radiology, Massachusetts General Hospital, Harvard Medical School, Boston, MA; [5]Memory Clinic, Department of Systems Medicine, University of Tor Vergata, Rome, Italy; and [6]Department of Neuroscience and Rehabilitation, University of Ferrara, Ferrara, Italy

ERP	event-related potential
GABA	Gamma-aminobutyric acid
GMFP	global mean field power
HVs	healthy volunteers
ICA	Independent Component Analysis
l-DLPFC	left dorsolateral prefrontal cortex
l-PPC	left posterior parietal cortex
LTD	long-term depression
LTP	long-term potentiation
MEG	magnetoencephalography
MEP	motor-evoked potential
M1	primary motor cortex
MMSE	Mini-Mental State Examination
MNI	Montreal Neurological Institute
MRI	magnetic resonance imaging
MT	motor threshold
PC	precuneus
PiB	Pittsburgh compound-B
PPC	posterior parietal cortex
SCD	scalp-to-cortex distance
SD	standard deviation
SV2A	synaptic vesicle protein 2A
TEP	TMS-evoked potential
TMS	transcranial magnetic stimulation

INTRODUCTION

In recent years, a growing body of evidence showed that alterations of the neuronal excitation/inhibition (E/I) imbalance can be a potential cause of neuronal network malfunctioning in Alzheimer's disease (AD), contributing to cognitive dysfunction.[1] In patients with AD, cortical activity has been investigated mainly with electrophysiological recordings, such as electroencephalographic (EEG) and magnetoencephalography (MEG),[2–4] and neuroimaging techniques, such magnetic resonance imaging (MRI).[5,6] However, all of these techniques present some limitations in detecting cortical activity dynamics. On one hand, EEG and MEG are not optimally tuned to record signals from specific cortical areas, because their spontaneous signals can be strongly affected by a blink or simple movement, which in-turn produces highly unstable responses in the spatial and frequency domain. On the other hand, neuroimaging techniques, although providing an accurate spatial resolution, can detect only slow changes in metabolic activity without an accurate reconstruction of the temporal dynamics in cortical activity. A more direct investigation of E/I imbalance can be achieved with transcranial magnetic stimulation (TMS). Preliminary findings obtained through the stimulation of the primary motor cortex (M1) and the simultaneous recording of motor-evoked potentials (MEPs) showed that motor threshold is abnormally increased in patients with AD.[7–12] Although consistent, these observations are confined to M1 and therefore cannot be informative of the neurophysiological state of associative cortical areas, which are directly affected during the disease progression.

In the present study, we used a novel approach consisting in applying TMS to frontal and parietal cortical areas while recording EEG activity from the scalp. In this manner, we could directly assess the excitability of these brain regions, using the stimulation-evoked post-synaptic potentials as a primary outcome measure.[13–18] Preliminary TMS-EEG studies in patients with AD focused on targeting the dorso-lateral prefrontal cortex (DLPFC) an area involved in AD pathology during the late stages of the disease, when frontal lobe-related symptoms become evident.[19,20] During the early stages of the disease, however, neuropathological abnormalities (ie, amyloid plaques and neurofibrillary tangles) involve mostly the posterior cortical regions of the brain, such as the posterior parietal cortex (PPC) and the precuneus (PC).[21] The PPC is an area strongly involved in AD pathophysiology.[22] Moreover, the PPC is frequently observed as an area of early hypometabolism, as detected by positron emission tomography (PET) fluorodeoxyglucose (FDG) imaging.[23] The PC is an area of early regional brain atrophy[24] and it is considered a vulnerable region for the transitional stage toward dementia, which may be targeted by tailored interventions.[25] Patients with AD often show a reduction of PC cortical thickness accompanied by an abnormal activation during memory tasks and decreased functional connectivity within the interconnected default mode network (DMN).[26] This is relevant because the activity of the PC is considered necessary for episodic memory retrieval, whose impairment represents the clinical onset of typical AD.[27,28]

In the current study, we applied TMS-EEG over the PC, the left DLPFC (l-DLPFC) and the left posterior parietal cortex (l-PPC). We hypothesized that TMS-EEG would show features of regional hyperexcitability that would be particularly evident in the PC, due to its key role in the early pathophysiology of AD. We also hypothesized that TMS-EEG cortical measures would be associated with the severity of cognitive impairment and with the underlying Aβ pathology.

Materials and Methods

Patients and Clinical Evaluation

A total of 65 patients with AD, admitted to the memory clinic of the Santa Lucia Foundation (Rome, Italy) between January 2014 and June 2020 were recruited for the current study. The study was approved by the review board and ethics committee of the Santa Lucia Foundation and was conducted following the

principles of the Declaration of Helsinki and the International Conference on Harmonization Good Clinical Practice guidelines. All patients or their relatives or legal representatives provided written informed consent. Patients could withdraw at any point without prejudice.

Patients were eligible if they had an established diagnosis of probable mild-to-moderate AD according to the International Working Group recommendations.[29] Inclusion criteria included: (1) patients with AD aged >50 to ≤85 years; (2) Mini-Mental State Examination (MMSE) score of 14 to 26 at screening; (3) one caregiver; and (4) had been treated with acetylcholinesterase inhibitor for at least 6 months. Patients were excluded if they had extrapyramidal signs, history of stroke, other neurodegenerative disorders, psychotic disorders, or if they had been treated 6 months before enrollment with antipsychotics, antiparkinsonian, anticholinergics, and anti-epileptic drugs. Signs of concomitant cerebrovascular disease on MRI scans (ie, major infarction, one strategic or multiple lacunar infarcts, extensive white matter lesions; one quarter of the total white matter) were carefully investigated and excluded in all patients. Patients who agreed to participate underwent a clinical evaluation with MMSE and a TMS-EEG evaluation to assess cortical excitability. Twenty-one age-matched healthy volunteers (HVs) were recruited after informed consent and underwent the same TMS-EEG evaluation as patients with AD.

Cortical Excitability Evaluation

Cortical excitability was assessed using single-pulse TMS during concomitant EEG recordings. During all the TMS-EEG recordings, participants sat on a comfortable armchair in a soundproof room in front of a computer screen. They were instructed to fixate on a white cross (6 × 6 cm) in the middle of the screen and to keep their arms rested in a relaxed position. During TMS-EEG, participants wore in-ear plugs which continuously played a white noise that reproduced the specific time-varying frequencies of the TMS click in order to mask the click and avoid possible auditory event-related potential (ERP) responses.[30] The intensity of the white noise was adjusted for each individual by increasing the volume (always below 90 decibels [dB]) until the participant was sure that s/he could no longer hear the TMS-induced click. TMS for EEG recordings was carried out using a Magstim Rapid^2 magnetic stimulator, which produces a biphasic waveform with a pulse width of ∼ 0.1 ms, connected to a figure-of-8 coil with a 70-mm diameter (Magstim Company, Whitland, UK).

The coil was differently oriented for the 3 areas of stimulation so that the direction of current flow in the most effective (second) phase was in a posterior–anterior direction. The 3 areas of stimulation were l-DLPFC, PC, and l-PPC. The order of stimulation to these areas was counterbalanced across patients. Individual T1-weighted MRI volumes were used as an anatomic reference. To target the l-DLPFC, the coil was positioned over the junction of the middle and anterior thirds of the middle frontal gyrus with an orientation of 45 degrees laterally. This positioning was based on previous studies using MRI-based neuronavigated TMS and TMS-EEG on this area,[19] corresponding to an area between the center of BA 9 and the border of BA 9 and 46 junctions. To target the PC, the coil was positioned along the medial superior parietal cortex with an orientation parallel to the midline.[18] To target the l-PPC, the coil was positioned over the angular gyrus, close to a posterior part of the adjoining caudal intraparietal sulcus with an orientation of 15 degrees from the midline.[18] Stimulation intensity for the 3 areas was based on a distance-adjusted motor threshold (adjMT) considering the individual scalp-to-cortex distance (SCD). The intensity of stimulation of single-pulse TMS was set at 90% of the adjMT. To ensure that this intensity was sufficient to evoke a reliable response in the patients with AD (ie. >40 V/m),[31] we computed the SCD value and the induced E-field over the TMS targets with SimNIBS version 3.2, an open-source simulation package that integrates segmentation of MRI scans, mesh generation, and FEM E-field computations.[32] For the HV group, we used the Montreal Neurological Institute (MNI) standard brain (ERNIE) provided in SimNIBS software as an anatomic reference. To ensure a high degree of reproducibility across neurophysiological assessments, the coil position was constantly monitored using the Softaxic neuronavigation system (E.M.S. Products, Bologna, Italy).

TMS was delivered in blocks of 120 single-pulses with a randomized inter-stimulus interval between 2 and 4 seconds. EEG was recorded with a TMS-compatible DC amplifier (BrainAmp; BrainProducts GmbH, Munich, Germany) from 29 TMS-compatible Ag/AgCl pellet electrodes mounted on an elastic cap. Additional electrodes were used as a ground and reference. The ground electrode was positioned in AFz, whrease the reference was positioned on the tip of the nose. EEG signals were digitized at a sampling rate of 5 kHz. Skin/electrode impedance was maintained below 5 kΩ. TMS-EEG data were preprocessed offline with Brain Vision Analyzer (Brain Products GmbH, Munich, Germany). Data were segmented into epochs starting 1 second before the TMS pulse and ending 1 second after it. TMS artifact was removed using cubic interpolation, from 1 ms before to 10 ms following the pulse. Data were then downsampled to 1,000 Hz and band-pass filtered between 1 and 80 Hz (Butterworth zero-phase filters). A 50 Hz notch filter was applied to reduce noise from electrical sources. Then, all the epochs were visually inspected and those with an excessively noisy EEG were excluded from the analysis. Independent component analysis (INFOMAX-ICA) was applied to the EEG signal to identify and remove components reflecting muscle activity, eye movements, blink-related activity, and residual TMS-related artifacts based on previously established criteria.[30,33] Finally, the signal was re-referenced to the average signal of all the electrodes.

EEG analysis was performed with MATLAB environment (version 2020; MathWorks Inc., Natick, MA, USA). Cortical excitability was assessed using TMS-evoked potentials (TEPs), computed by averaging all the time-locked EEG responses in each electrode, from 100 ms before to 300 ms after the TMS pulse, with a baseline correction of 100 ms before the TMS pulse.

Statistical Analysis

Prior to undergoing parametric or nonparametric statistical procedures, assumption of normality distribution of data residuals was

assessed with Shapiro-Wilks' test; and the assumption of homoscedasticity was assessed with Levene's test. For linear regression analyses, assumption of multicollinearity among predictors was assessed by means of the variance inflation factor. Assumption of independence of residuals was assessed by means of the Durbin-Watson test. Level of significance was set at $\alpha = 0.05$.

A first set of analyses was aimed at comparing demographics (ie, sex, age and education, and baseline characteristics; ie, MMSE score, resting motor threshold (RMT), SCD, and E-field, of the AD and HV groups. This analysis was conducted with unpaired *t* tests or Pearson's chi-square test (for the categorical variable sex). We then assessed differences in cortical excitability, measured with TEPs, between the 2 groups (patients with AD vs HVs) both at the global level (ie, comparing TEPs over all the scalp), and at the local level (ie, comparing TEPs over the site of stimulation). Analysis of cortical excitability at the global level was performed with nonparametric, cluster-based permutation statistics comparing the 2 groups, at each electrode at specific time windows: 10 to 20 ms, 20 to 45 ms, 45 to 70 ms, and 70 to 130 ms; these time windows were based on the visual inspection of each TEP waveform and were consistent with previous investigations.[18,34,35] Given the very high number of comparisons (2 groups × 29 electrodes × 4 time windows), to reduce the occurrence of false I type errors, this method calculates Monte Carlo estimates of the significance probabilities from 2 surrogate distributions constructed by randomly permuting the 2 original conditions data for 3,000 times. The clusters for permutation analysis were defined as the 2 (or more) neighboring electrodes in which the statistic value at a given timepoint exceeded the significance threshold.[36] Analysis of cortical excitability locally to the stimulated area was performed with multiple independent *t* tests comparing the TEP waveform recorded at the closest electrode to the stimulation (F3 for l-DLPFC, Pz for PC, and P3 for l-PPC) in the 2 groups (patients with AD vs HVs). Given the high number of comparisons (2 groups × 4 time windows) To avoid the occurrence of false I type errors, this analysis was performed by permuting the original distributions 3,000 times and correcting the *p* values with the false discovery rate method. The same analysis was conducted to assess whether there was any difference in the TMS-evoked activity after sham stimulation between the 2 groups (patients with AD vs HVs).

The second set of analyses was aimed at testing the predictive value of the level of cortical excitability at the cognitive/behavioral level of patients with AD. This analysis was conducted by using a stepwise backward linear regression with the MMSE score as the dependent variable. The predictor variables of the model were the amplitude of the early TEP peak evoked within the first 30 ms after TMS of the 3 stimulated areas.

The third set of analyses was aimed at exploring the linear relationships between the level of cortical excitability (ie, the amplitude of the early TEP peak evoked in each area within the first 30 ms), and the level of CSF tau, p-tau, and $A\beta_{42}$. This analysis was conducted by using Pearson's correlation coefficient. Given the high number of correlations (3 areas × 3 cerebrospinal fluid [CSF] level), to avoid the occurrence of false I type errors, we corrected the *p* values with the false discovery rate method.

Results

The baseline patients with AD and HVs' characteristics are shown in the . The mean age of the total sample of patients with AD was 73.96 years (SD = 5.98, ranging from 60 to 88), of which 64% were women (n = 42), whereas the mean age of the HV group was 71.21 years (SD = 6.32, ranging from 60 to 82 years). No differences in sex, age, or education years were found (all *p* values >0.05). The mean MMSE raw score at baseline was 22.05 (SD = 3.23) for the patients with AD and 28.81 (SD = 1.86) for the HVs. The mean RMT (percentage of maximal stimulator output) was 51.89 (SD = 8.78) in the AD group and 58.25 (SD = 5.70) in the HV group. RMT values were lower in the patients with AD compared with the HV group ($p < 0.05$). The entire procedure was well-tolerated with no reports of adverse effects.

Figure 1 depicts the coil positioning and e-field induced over the 3 targets of stimulation. To ensure that the three TMS targets receive the same stimulation in terms of efficacy and intensity, we first computed the SCD for the 3 areas obtaining the following results: 18.95 ± 2.5 mm for the l-DLPFC; 24.9 ± 1.7 mm for the PC; and 21.3 ± 4.8 mm for the l-PPC. We then computed the difference between the SCD in the AD group and the standard SCD values used for the HV group in the 3 areas (l-DLPFC-SCD difference = 5.43 ± 2.11 mm; PC-SCD difference = 5.43 ± 1.92 mm; and l-PPC-SCD difference = 5.83 ± 3.41 mm) without observing any difference among the 3 SCD (l-DLPFC vs PC: $p = 0.9$; l-DLPFC vs l-PPC: $p = 0.6$; and PC vs l-PPC: $p = 0.7$). All of our participants received a stimulation of at least 45 V/m (mean 61 ± 5.21 V/m) with no differences in the e-field induced in the 3 TMS spots (all *p* values > 0.05) and no differences compared to the e-fields estimated for the HV group using the standard brain (all *p* values > 0.05).

Figures 2 to 4 show the spatio-temporal reconstruction of TEPs recorded over all the scalp after stimulation of the l-DLPFC (see Fig 2), PC (see Fig 3), and l-PPC (see Fig 4). Regardless of the stimulation site, single-pulse TMS evoked a well-known pattern of 5 main peaks of activity, lasting around 250 ms: P30, N45, P60-65, N100, and P180. The spatio-temporal reconstruction of these components followed a similar dynamic among the 3 areas of stimulation with a prominent activity focused on the stimulated area (15–40 ms) that subsequently spread intra- and inter-hemispherically (60–120 ms), and finally resulted in a central positivity, namely P180, which is known to be produced by a TMS-evoked auditory artifact,[30] for this reason, this last peak was not included in the analysis.

Analysis of TEPs at the global level was first conducted to assess differences in cortical excitability throughout the

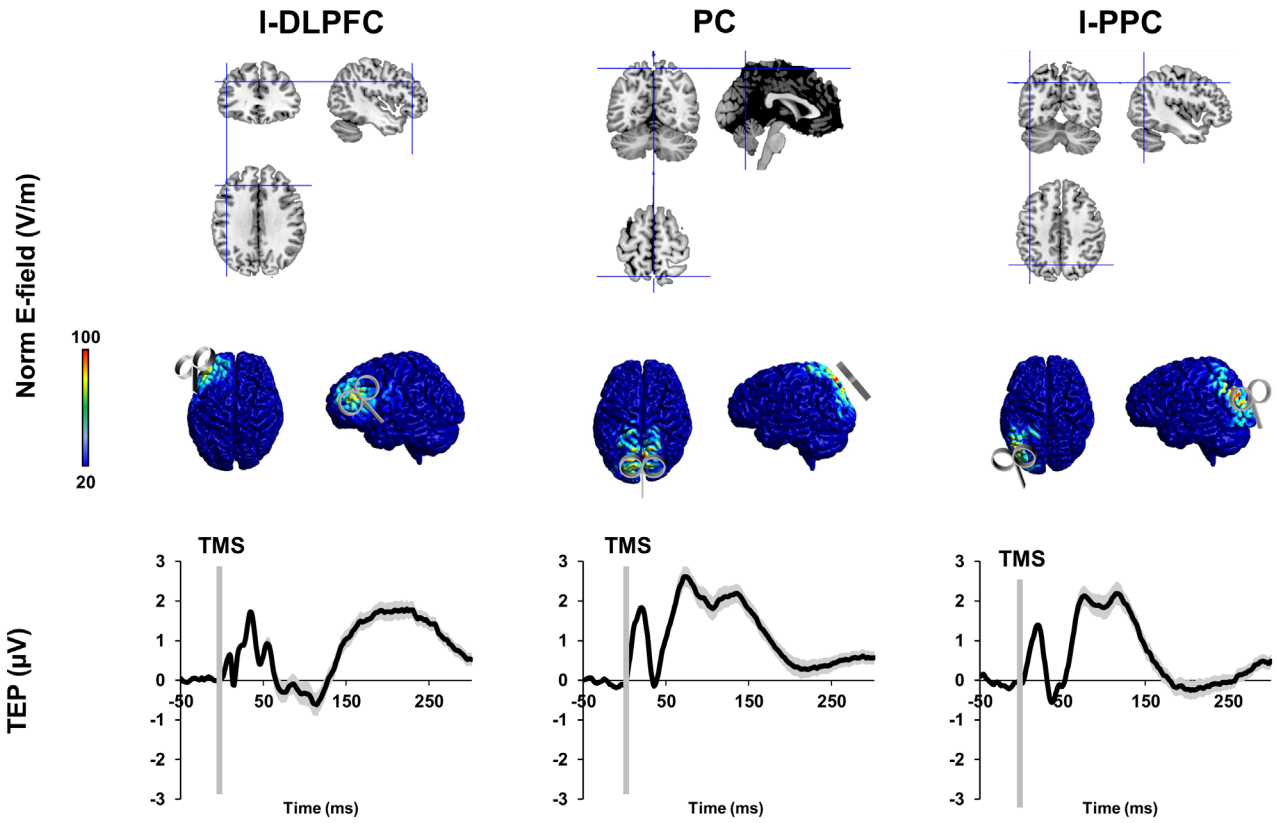

FIGURE 1: Schematic representation of the cortical excitability evaluation. Each patient underwent 3 simultaneous transcranial magnetic stimulation and electroencephalographic (TMS-EEG) recordings over the left dorso-lateral prefrontal cortex (l-DLPFC), the precuneus (PC), and the left posterior parietal cortex (l-PPC). Individual T1-weighted magnetic resonance imaging (MRI) volumes were used as an anatomic reference. For each stimulation we estimated the electric field (e-field) induced in the cortex. Each TMS-EEG recording comprised 120 TMS single-pulses resulting in a TMS-evoked potential (TEP) analyzed as a measure of cortical excitability.

TABLE. Patients with Alzheimer's Disease (AD) and Healthy Volunteers (HVs) Demographics and Clinical Characteristics at Baseline

	Patients with AD (n = 65)	HV (n = 21)	*p* value
Age, yr, mean (SD)	73.96 (5.98)	71.21 (6.32)	$p > 0.05$
Sex, women, number (%)	42 (64%)	12 (57%)	$p > 0.05$
Education, yr, mean (SD)	8.39 (3.99)	10.04 (4.98)	$p > 0.05$
RMT, % stimulator output, mean (SD)	51.89 (8.78)	58.25 (5.70)	$p < 0.05$*
Proportion of patients taking cholinesterase inhibitors, number (%)	50 (76%)		
Proportion of patients taking memantine, number (%)	13 (20%)		
APOE e4 carrier, number (%)	33 (52%)	-	-
MMSE raw score, mean (SD)	22.05 (3.23)	28.81 (1.86)	$p < 0.05$*

Abbreviation: AD = Alzheimer's disease; HV = healthy volunteers; MMSE = Mini Mental State Examination; RMT = resting motor threshold.

entire scalp between the AD and the HV groups. When stimulated over the l-DLPFC (see Fig 2A), the patients with AD showed higher cortical excitability between 20 and 40 ms after TMS, over a cluster of 2 left frontal electrodes (all Monte Carlo p values < 0.01) and over a cluster of right posterior electrodes (all Monte Carlo p values < 0.01). When

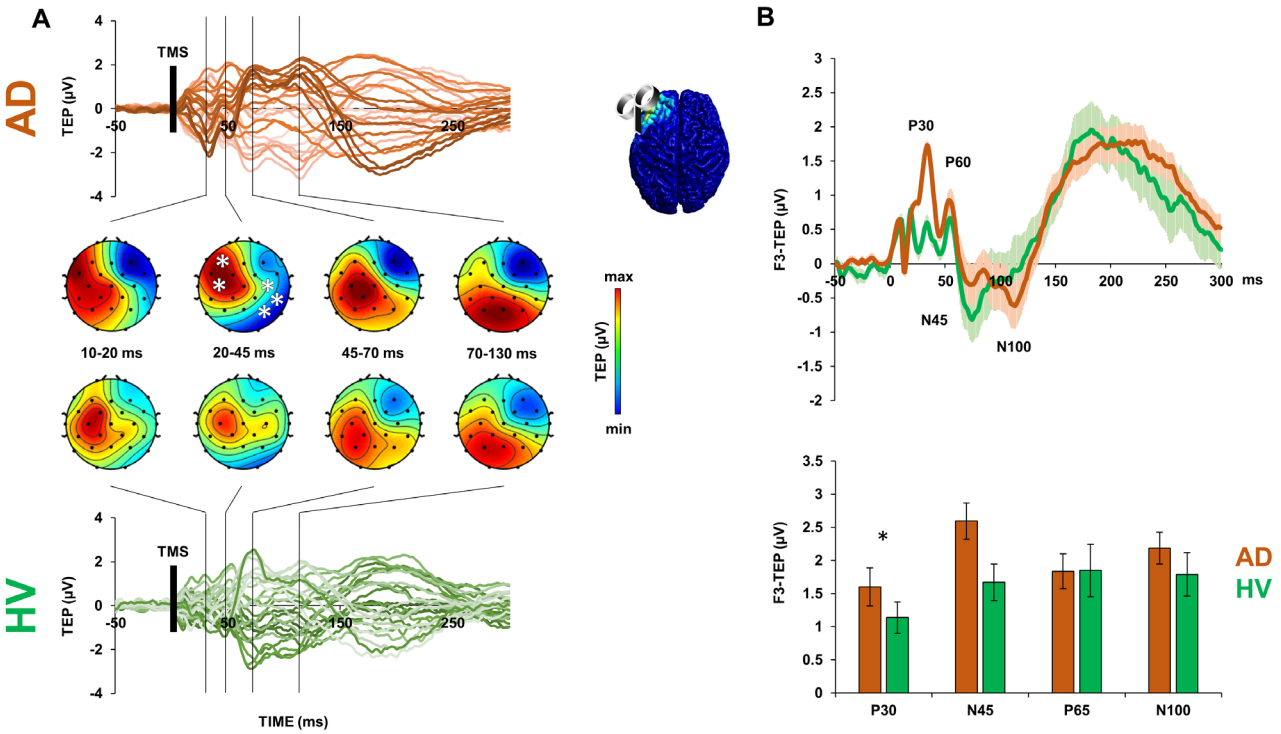

FIGURE 2: Cortical excitability analysis after left dorso-lateral prefrontal cortex stimulation. (A) Transcranial magnetic stimulation (TMS)-evoked potentials (TEPs) recorded over all the scalp after stimulation of the left dorso-lateral prefrontal cortex (l-DLPFC) in the Alzheimer's disease (AD) group (upper panel) and in the healthy volunteers (HVs) group (lower panel). Scalp maps depict the voltage distribution in the specified time windows. (B) TEPs recorded over the l-DLPFC in the AD group and in the HV group. Error bars and shaded lines indicate standard error. * Indicates $p < 0.05$.

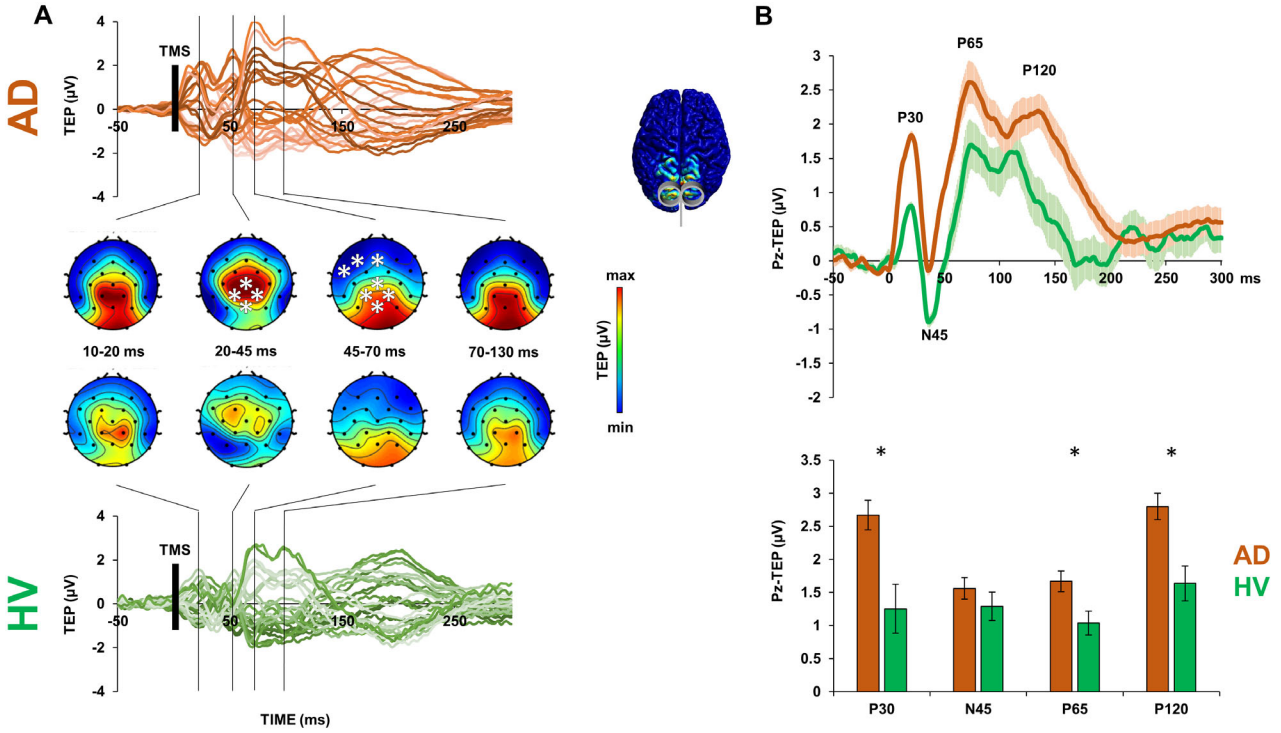

FIGURE 3: Cortical excitability analysis after precuneus stimulation. (A) Transcranial magnetic stimulation (TMS)-evoked potentials (TEPs) recorded over all the scalp after stimulation of the precuneus (PC) in the Alzheimer's disease (AD) group (upper panel) and in the healthy volunteers (HVs) group (lower). Scalp maps depict the voltage distribution in the specified time windows. (B) TEPs recorded over the PC in the AD group and in the HV group. Error bars and shaded lines indicate standard error. * Indicates $p < 0.05$.

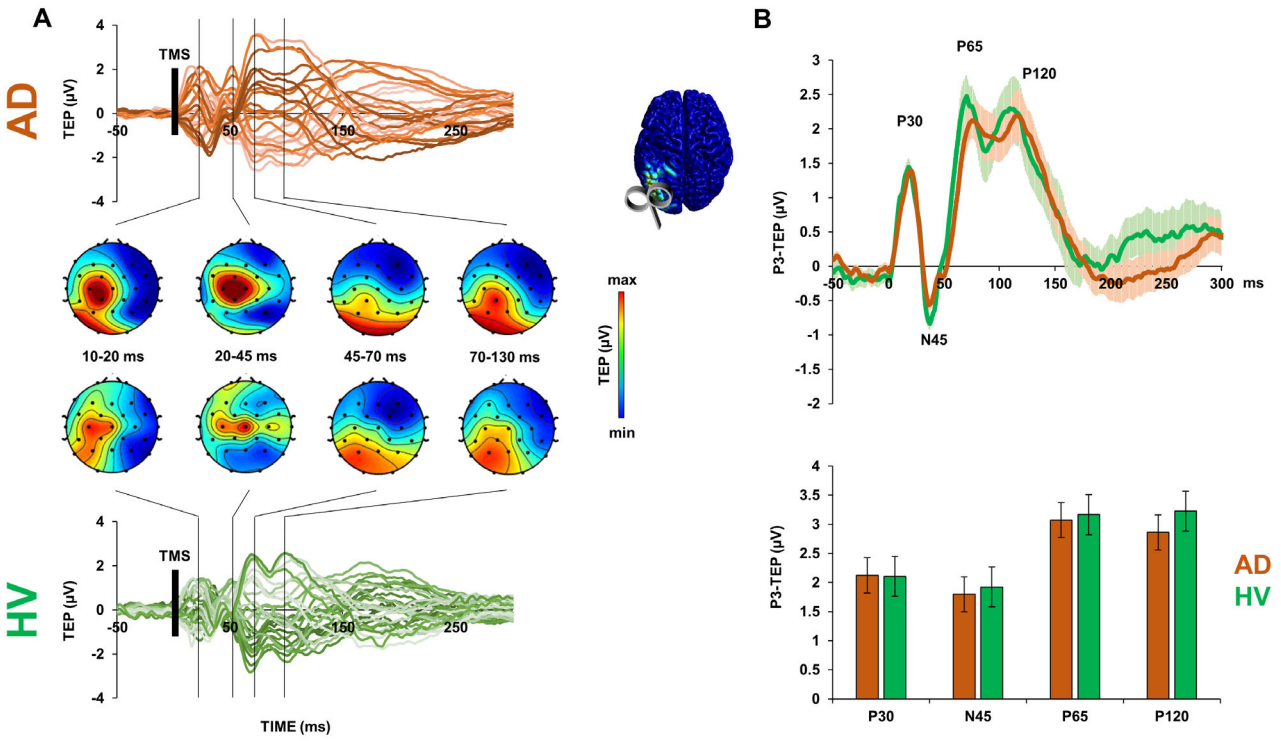

FIGURE 4: Cortical excitability analysis after left posterior parietal cortex stimulation. (A) Transcranial magnetic stimulation (TMS)-evoked potentials (TEPs) recorded over all the scalp after stimulation of the left posterior parietal cortex (l-PPC) in the Alzheimer's disease (AD) group (upper panel) and in the healthy volunteers (HVs) group (lower panel). Scalp maps depict the voltage distribution in the specified time windows. (B) TEPs recorded over l-PPC in the AD group and in the HV group. Error bars and shaded lines indicate standard error. * Indicates $p < 0.05$.

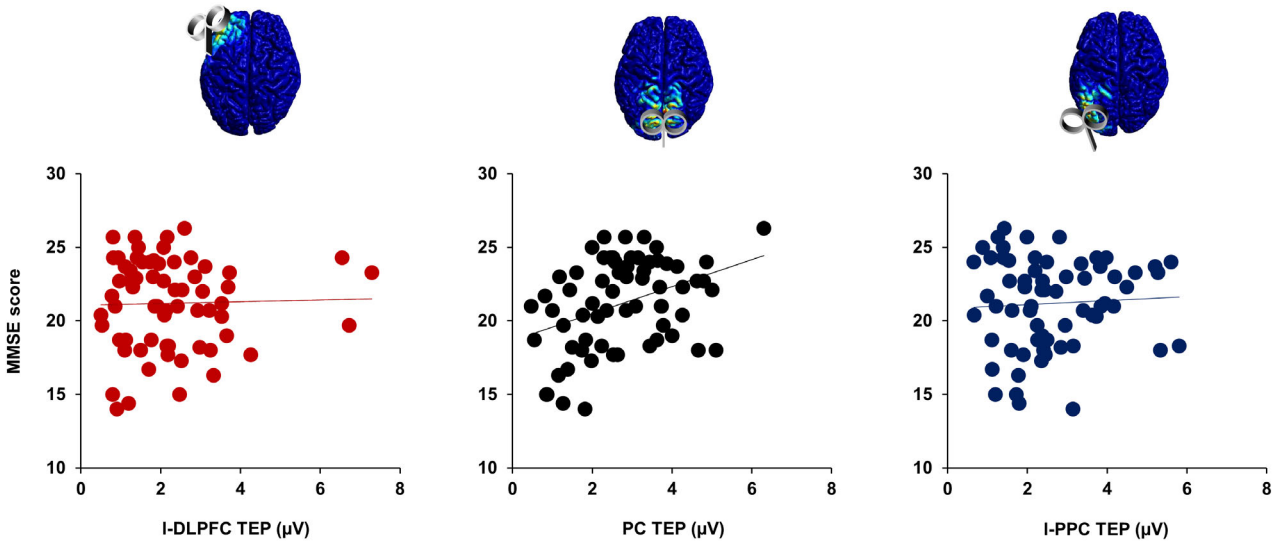

FIGURE 5: Linear relationships between cortical excitability and cognitive level. Scatterplots depicting the linear relationship between the Mini Mental State Examination (MMSE) score (y-axis) and the general amplitude of the transcranial magnetic stimulation (TMS)-evoked potential (TEP) recorded over the left dorso-lateral prefrontal cortex (l-DLPFC, left plot), the precuneus (PC, central plot), and the left posterior parietal cortex (l-PPC, right plot).

stimulated over the PC (see Fig 3A), patients with AD showed higher cortical excitability between 30 and 50 ms after TMS, over a cluster of 4 electrodes locally to the stimulated medial parietal area (all Monte Carlo p values < 0.01); and in a subsequent temporal window between 50 and 90 ms over 2 clusters of electrodes, 1 of 4 electrodes over the stimulated area, and 1 of 3 frontal electrodes (all Monte Carlo p values < 0.01). No differences were observable when the 2 groups were stimulated over the l-PPC (see Fig 4A; all Monte Carlo p values > 0.05).

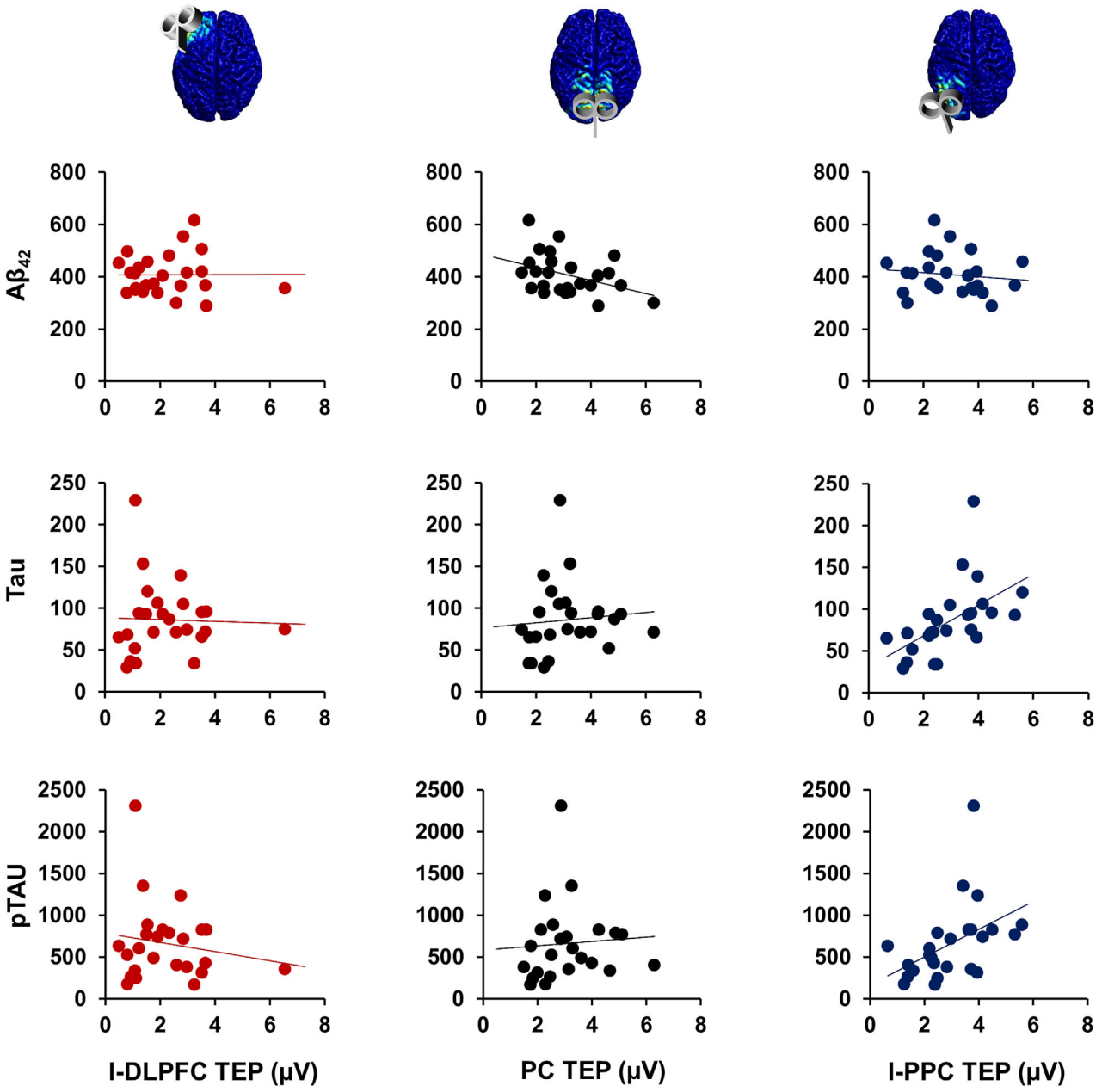

FIGURE 6: Linear relationships between cortical excitability and cerebrospinal fluid biomarkers. Scatterplots depicting the linear relationship between the level of amyloid beta ($A\beta_{42}$; upper plots), tau (central plots), and p-tau (below plots; y-axis) and the general amplitude of the TMS-evoked potential (TEP) recorded over the left dorso-lateral prefrontal cortex (l-DLPFC, left plots), the precuneus (PC, central plots), and the left posterior parietal cortex (l-PPC, right plots).

To compare the reactivity of the stimulated area between the AD and the HV groups, we subsequently performed a temporal analysis of the TEP evoked at the local level. Panel B of Figures 2 to 4 show the local TEP waveform recorded over the closest electrode of the stimulated area: F3 for l-DLPFC stimulation, Pz for PC stimulation, and P3 for l-PPC stimulation. When stimulated over the l-DLPFC, the AD group showed a higher TEP amplitude between 20 and 40 ms when compared to the HV group (AD = 1.602 ± 0.286 and HV = 1.137 ± 0.235; t = 2.370, p = 0.021; see Fig 2B). When stimulated over the PC, patients with AD showed a higher TEP amplitude that was evident in all time windows, between 10 and 30 ms (AD = 2.671 ± 0.222 and HV = 1.252 ± 0.368; t = 3.263, p = 0.002), between 50 and 90 ms (AD = 1.671 ± 0.156 and HV = 1.038 ± 0.182; t = 2.208, p = 0.03), and between 90 and 160 ms (AD = 2.801 ± 0.201 and HV = 1.637 ± 0.264; t = 3.118, p = 0.003; see Fig 3B). No differences were observable between the TEP of the 2 groups when stimulated over the l-PPC (all p values > 0.05; see Fig 4B).

A total of 33 patients screened positive as carriers for at least one APOE ε4 allele. There were no differences as compared with APOE3 carriers in any of the neurophysiological measures we tested (all p values > 0.05).

Figure 5 depicts the linear relationships between the TEP amplitude evoked in the 3 areas and the MMSE score. Backward stepwise regression analysis showed that PC-TEP was the only neurophysiological parameter associated with cognitive impairment, as measured with MMSE ($\beta = 0.924 \pm 0.28$; standardized $\beta = 0.382$; $p = 0.002$) whereas l-DLPFC-TEP and l-PPC-TEP were not significant (all p values > 0.05).

CSF tau, p-tau, and the Aβ42 levels were available in 25 patients with AD. CSF levels of Aß42 and Aß40, CSF t-tau, and p-tau phosphorylated at Thr181 concentrations were determined using a sandwich enzyme-linked immunosorbent assay (EUROIMMUN ELISA). Figure 6 depicts the linear relationships between the TEP amplitude evoked in the 3 areas and the levels of $A\beta_{42}$, tau, and p-tau. Correlation analyses revealed that the amplitude of the first PC-TEP peak and levels of $A\beta_{42}$ were negatively correlated ($r = -0.391$, $p = 0.026$), whereas the amplitude of the first l-PPC-TEP peak was positively correlated with levels of tau ($r = 0.458$, $p = 0.011$) and p-tau ($r = 0.544$, $p = 0.002$).

Discussion

The current set of results highlights the presence of regional hyperexcitability over the PC in patients with mild-to-moderate AD. This finding was directly observable by recording EEG from the scalp while stimulating the PC with TMS in a large sample of patients with AD, which were compared with a group of age-matched HVs. Moreover, the individual level of cortical excitability over the PC, as measured with the first TEP peak amplitude, was predictive of the degree of patient's cognitive impairment, as measured with the MMSE score. Finally, we found a linear correlation between the individual level of cortical excitability and CSF biomarkers. Specifically, patients who showed higher PC excitability were the ones who had lower CSF levels of $A\beta_{42}$.

There is substantial mechanistic evidence that neuronal hyperactivity can be directly mediated by soluble Aβ, which is highly enriched around amyloid plaques.[37] This is supported by experimental findings showing that local application of soluble Aβ to neuronal circuits in vivo induces hyperactivity and that suppression of Aβ production by beta- or gamma-secretase inhibition blocks hyperactivity.[38] Mechanistically, the link between Aβ and hyperexcitability has been attributed to an Aβ-dependent shift in E/I balance, favoring excitation (eg, through inhibition of glutamate reuptake).[37] Although multiple neurotransmitter systems are involved, previous studies showed that neurotransmission of the PC is mainly driven by cholinergic receptors. The parietal cortex receives cholinergic innervation from select subfields of the nucleus basalis, which is important in cognitive functions.[39] Accordingly, it has been shown that AD-related atrophy, in particular in the PC and hippocampus, dramatically affects the cholinergic system.[40] Here, the depository of amyloid and plaque formation causes an impairment of the cholinergic transmission,[41] which leads in turn to memory loss and cognitive impairment.[39] The oligomeric form of Aβ interacting with α7-containing nicotinic acetylcholine receptor (nAChR) subtypes of the nucleus basalis, lead to enhanced neuronal intrinsic excitability and action potential firing rates.[42] Moreover, PC choline acetyltransferase (ChAT) activity decreases in parallel with increases in Pittsburgh compound-B (PiB) binding and soluble Aβ concentration.[43] As a high number of cholinergic receptors are found in the medial parietal region, and in particular in the PC, a deficit of these receptors due to Aβ pathology could affect the excitability threshold of the PC, likely explaining why our results showed an abnormally higher TEP amplitude over the stimulated area. This novel finding is consistent with our initial hypothesis, which considered the PC as central brain region involved in AD pathological dysfunction, due to previous work showing that the PC has the highest initial level of Aβ.[26] This hypothesis was further confirmed by another finding in this study, demonstrating that TEP amplitude recorded over the PC correlated with the levels of CSF Aβ, but not with CSF tau or p-tau levels. The relation is indicative of PC hyperexcitability as a consequence of the underlying Aβ pathology.

Another important finding of the present study is the observed association between the individual levels of PC excitability and the severity of cognitive impairment. Specifically, patients showing a higher level of PC excitability were the ones with a higher initial MMSE score. Although this result seems in contrast with the hypothesis of dysfunctional hyperexcitability, it is possible that this phenomenon may reflect underlying compensatory mechanisms that are attempting to preserve cognitive abilities in the early phases of AD due to the underlying Aβ pathology. Hyperexcitability has been constantly described in TMS studies evaluating M1, with a large body of evidence reporting increased cortical excitability.[8-12] The increase in cortex excitability, however, does not appear correlated to underlying structural changes,[44] overall suggesting that pathophysiological mechanisms underlying cortex hyperexcitability in AD might be different and independent from those associated with cortical atrophy and degeneration of fiber tracts.

Hyperexcitability might indeed be interpreted as a protective mechanism counteracting the underlying Aβ mediated cholinergic dysfunction.

A growing body of evidence points toward the PC as an ideal target for interventions to slow down and potentially counteract the memory decline in patients with AD.[18,45,46] This hypothesis is supported by recent experimental works showing that repetitive TMS (rTMS) applied to the PC is effective in modulating long-term memory functions[45] and connectivity with the temporal cortex in the healthy brain.[46] Along the same lines, we have recently demonstrated that a 2-week course of 20-Hz rTMS over the PC improves long-term memory in patients with AD, providing key preliminary evidence that PC stimulation is a viable strategy to improve cognitive dysfunction in AD.[18] This result has been recently confirmed by the first long-term 24 weeks, phase II, randomized-controlled trial in which we reported safety and efficacy of rTMS over the PC in reducing functional and cognitive decline in a sample of 50 patients with AD (NCT03778151).[47] Hence, the current findings may be important for future studies to consider, as they can better stratify patients with AD and evaluate potential responses to therapy in the context of clinical applications based on neurostimulation.

We also found that the prefrontal cortex in patients with AD is characterized by hyperexcitability, although to a lesser extent. Indeed, when compared to HVs, stimulation of the l-DLPFC in patients with AD revealed a higher amplitude of a specific early TEP component, peaking at 30 ms (P30). Interestingly, previous TMS-EEG studies in patients with AD have also shown an altered P30 response when targeting either the motor cortex[14] or the DLPFC.[15] The origin of the P30 potential is not entirely clear, but it has been suggested that gamma-aminobutyric acid (GABA-A) postsynaptic receptors are involved in the generation and modulation of this TEP peak.[16,48] It is important to note that we did not find any significant correlation between the observed prefrontal hyperexcitability and clinical severity, thereby limiting the importance of this finding when put in the clinical context. This result is in contrast to a recent study, which found a link between hyperexcitability and clinical severity, however, in patients at later stages of the disease.[15] Hence, it may be that prefrontal hyperexcitability becomes more evident when the disease progresses. Similarly, the absence of linear relationships among DLPFC hyperexcitability and CSF Aβ, tau, and p-tau levels made it not possible to ascribe such phenomenon to any clear underlying pathological mechanism.

A different result was obtained after stimulation of the l-PPC. However, we observed a perfect overlapping between the l-PPC-TEP of the 2 groups, with no difference in their spatiotemporal distribution, suggesting that this area could be differently involved in the pathophysiology of AD. In general, Aβ seems to accumulate mainly in posterior hubs that show high structural and functional connectivity within the DMN, such as the PC.[49] In addition, the pattern of Aβ accumulation differs from that of tau. The progressive deposition of tau spreads from the middle temporal lobe to the inferolateral temporal lobe and then to the medial and lateral parietal lobes,[22] in a distribution that largely recapitulates Braak neuropathological staging.[50] According to this different spread of pathological tau deposits through the course of AD, we found that l-PPC TEP amplitude, although not differing from HVs, was correlated with CSF levels of tau and p-tau, but not with Aβ CSF levels. Further studies considering metabolic, tau, and Aβ imaging with TMS-EEG are needed to better understand the possible correlation between regional cortical hyperexcitability and the underlying pathological accumulation of tau and Aβ, as compared to regional hypometabolism.

Our findings point to the TMS-EEG approach as a powerful technique to measure cortical activity in AD, as we previously suggested in other works.[18,19,51] Cortical excitability was assessed by monitoring TEPs, whose amplitude and spatiotemporal distribution reflect the neurophysiological state of the stimulated area.[16,35] Although the exact nature of TEPs have not been fully elucidated, it has been suggested that, when tested in the primary motor cortex, early peaks (between 7 and 30 ms) reflect local excitability of the stimulated area being sensitive to its level of activation,[52] functional state,[53] and intensity of stimulation.[54] From a physiological point of view, early TEPs are thought to reflect glutamate-mediated excitatory post-synaptic potentials, representing a direct index of local excitability.[55-57] Later TEPs, from 30 to 70 ms and from 70 to 180 ms, may reflect $GABA_A$ and $GABA_B$-mediated inhibitory post-synaptic potentials.[56,58,59] In our study, analysis of PC TEPs showed a consistent regional hyperexcitability in patients with AD evident across the 3 main peaks analyzed. Because there were no specific differences among the different peaks' components, such hyperexcitability is not likely related to a specific glutamatergic or GABAergic deficit. Further studies are needed to better understand the possible relationship among the described hyperexcitability and the underlying synaptic dysfunction.

A further main limitation of this technique lies in the TMS-evoked nonspecific effects, such as auditory and somatosensory responses, that can affect the late EEG response (ie, after 100 ms from TMS).[30,60] In this regard, we restricted our analysis to the first 130 ms after the TMS

pulse where, with an adequate stimulation of the cortex, only the cortical TEPs are evoked.[30] Here, to ensure an appropriate stimulation of the cortex, we optimized our TMS-EEG approach so that each stimulation parameter was set based on the individual brain anatomy of the patients with AD. Unfortunately, we did not have individual MRI scans for the HV group. Thus, we could not test for possible differences in the scalp-to-cortex distance between the 2 groups that could have driven our results. However, this hypothesis is very unlikely because there were no differences in the induced e-field used to stimulate the 3 areas, and no difference in the SCD of the 3 areas computed relative to the standard values used for HV group. It is also important to note that the localization procedure we performed to target the PC was based on previous studies of group using TMS or rTMS over the PC,[18,45,46,51] although some studies reported a more inferior[26,61] or superior site.[62,63]

In conclusion, our data reveal that patients with AD are characterized by striking hyperexcitability within the PC and, to some extent, over the frontal lobe, confirming the findings reported in neuroimaging studies. Moreover, our results point to TMS-EEG as a novel method to measure regional E/I unbalance in a direct and noninvasive way through the spatiotemporal analysis of TEPs.

Acknowledgments

The authors would like to thank all the patients that took part in this study and their families. G.K. received funding from the Italian Ministry of Health, the Alzheimer's Drug Discovery Foundation and the European Research Council (Neurotwin) and the BrightFocus Foundation (grant number A2019523S). E.P.C. received a "Be-for-ERC" funding from La Sapienza University. Open access funding provided by BIBLIOSAN.

Author Contributions

G.K. and E.P.C. participated in the study concept and design. E.P.C., I.B., S.B., M.A., M.M., M.C.P., A.D., L.M., F.D.L., and M.M. acquired and analyzed the data. G.K., E.P.C., and D.A.S. contributed to drafting the text or preparing the figures.

Potential Conflicts of Interest

Nothing to report.

References

1. Maestú F, de Haan W, Busche MA, DeFelipe J. Neuronal excitation/inhibition imbalance: core element of a translational perspective on Alzheimer pathophysiology. Ageing Res Rev 2021;69:101372. https://doi.org/10.1016/j.arr.2021.101372.
2. Ranasinghe KG, Kudo K, Hinkley L, et al. Neuronal synchrony abnormalities associated with subclinical epileptiform activity in early-onset Alzheimer's disease. Brain 2022;145:744–753. https://doi.org/10.1093/brain/awab442.
3. Lam AD, Sarkis RA, Pellerin KR, et al. Association of epileptiform abnormalities and seizures in Alzheimer disease. Neurology 2020;95:e2259–e2270. https://doi.org/10.1212/WNL.0000000000010612.
4. Babiloni C, Arakaki X, Azami H, et al. Measures of resting state EEG rhythms for clinical trials in Alzheimer's disease: recommendations of an expert panel. Alzheimers Dement 2021;17:1528–1553. https://doi.org/10.1002/alz.12311.
5. Teipel SJ, Grothe M, Lista S, et al. Relevance of magnetic resonance imaging for early detection and diagnosis of Alzheimer disease. Med Clin 2013;97:399–424. https://doi.org/10.1016/j.mcna.2012.12.013.
6. Davatzikos C, Fan Y, Wu X, et al. Detection of prodromal Alzheimer's disease via pattern classification of magnetic resonance imaging. Neurobiol Aging 2008;29:514–523. https://doi.org/10.1016/j.neurobiolaging.2006.11.010.
7. Alagona G, Ferri R, Pennisi G, et al. Motor cortex excitability in Alzheimer's disease and in subcortical ischemic vascular dementia. Neurosci Lett 2004;362:95–98. https://doi.org/10.1016/j.neulet.2004.03.006.
8. de Carvalho M, de Mendonça A, Miranda PC, et al. Magnetic stimulation in Alzheimer's disease. J Neurol 1997;244:304–307. https://doi.org/10.1007/s004150050091.
9. Alagona G, Bella R, Ferri R, et al. Transcranial magnetic stimulation in Alzheimer disease: motor cortex excitability and cognitive severity. Neurosci Lett 2001;314:57–60. https://doi.org/10.1016/S0304-3940(01)02288-1.
10. Lazzaro VD, Oliviero A, Pilato F, et al. Motor cortex hyperexcitability to transcranial magnetic stimulation in Alzheimer's disease. J Neurol Neurosurg Psychiatry 2004;75:555–559. https://doi.org/10.1136/jnnp.2003.018127.
11. Martorana A, Stefani A, Palmieri MG, et al. L-dopa modulates motor cortex excitability in Alzheimer's disease patients. J Neural Transm 2008;115:1313–1319. https://doi.org/10.1007/s00702-008-0082-z.
12. Khedr EM, Ahmed MA, Darwish ES, Ali AM. The relationship between motor cortex excitability and severity of Alzheimer's disease: a transcranial magnetic stimulation study. Clin Neurophysiol 2011;41:107–113. https://doi.org/10.1016/j.neucli.2011.03.002.
13. Casarotto S, Määttä S, Herukka SK, et al. Transcranial magnetic stimulation-evoked EEG/cortical potentials in physiological and pathological aging. Neuroreport 2011;22:592–597. https://doi.org/10.1097/WNR.0b013e328349433a.
14. Ferreri F, Vecchio F, Vollero L, et al. Sensorimotor cortex excitability and connectivity in Alzheimer's disease: a TMS-EEG co-registration study. Hum Brain Mapp 2016;37:2083–2096.
15. Bagattini C, Mutanen TP, Fracassi C, et al. Predicting Alzheimer's disease severity by means of TMS–EEG coregistration. Neurobiol Aging 2019;80:38–45.
16. Tremblay S, Rogasch NC, Premoli I, et al. Clinical utility and prospective of TMS–EEG. Clin Neurophysiol 2019;130:802–844. https://doi.org/10.1016/j.clinph.2019.01.001.
17. Casula EP, Pellicciari MC, Bonnì S, et al. Evidence for interhemispheric imbalance in stroke patients as revealed by combining transcranial magnetic stimulation and electroencephalography. Hum Brain Mapp 2021;42:1343–1358. https://doi.org/10.1002/hbm.25297.
18. Koch G, Bonnì S, Pellicciari MC, et al. Transcranial magnetic stimulation of the precuneus enhances memory and neural activity in prodromal Alzheimer's disease. Neuroimage 2018;169:302–311.
19. Koch G, Motta C, Bonnì S, et al. Effect of rotigotine vs placebo on cognitive functions among patients with mild to moderate Alzheimer disease: a randomized clinical trial. JAMA Netw Open 2020;3:e2010372. https://doi.org/10.1001/jamanetworkopen.2020.10372.

20. Martorana A, Koch G. Is dopamine involved in Alzheimer's disease? Front Aging Neurosci 2014;6:252. https://doi.org/10.3389/fnagi.2014.00252.

21. Buckner RL, Snyder AZ, Shannon BJ, et al. Molecular, structural, and functional characterization of Alzheimer's disease: evidence for a relationship between default activity, amyloid, and memory. J Neurosci 2005;25:7709–7717. https://doi.org/10.1523/JNEUROSCI.2177-05.2005.

22. Jagust W. Imaging the evolution and pathophysiology of Alzheimer disease. Nat Rev Neurosci 2018;19:687–700. https://doi.org/10.1038/s41583-018-0067-3.

23. Herholz K, Salmon E, Perani D, et al. Discrimination between Alzheimer dementia and controls by automated analysis of multicenter FDG PET. Neuroimage 2002;17:302–316. https://doi.org/10.1006/nimg.2002.1208.

24. Gili T, Cercignani M, Serra L, et al. Regional brain atrophy and functional disconnection across Alzheimer's disease evolution. J Neurol Neurosurg Psychiatry 2011;82:58–66. https://doi.org/10.1136/jnnp.2009.199935.

25. Canter RG, Penney J, Tsai LH. The road to restoring neural circuits for the treatment of Alzheimer's disease. Nature 2016;539:187–196. https://doi.org/10.1038/nature20412.

26. Karas G, Scheltens P, Rombouts S, et al. Precuneus atrophy in early-onset Alzheimer's disease: a morphometric structural MRI study. Neuroradiology 2007;49:967–976. https://doi.org/10.1007/s00234-007-0269-2.

27. Lundstrom BN, Ingvar M, Petersson KM. The role of precuneus and left inferior frontal cortex during source memory episodic retrieval. Neuroimage 2005;27:824–834. https://doi.org/10.1016/j.neuroimage.2005.05.008.

28. Bonanni L, Moretti D, Benussi A, et al. Hyperconnectivity in dementia is early and focal and wanes with progression. Cereb Cortex 2021;31:97–105. https://doi.org/10.1093/cercor/bhaa209.

29. Dubois B, Hampel H, Feldman HH, et al. Preclinical Alzheimer's disease: definition, natural history, and diagnostic criteria. Alzheimers Dement 2016;12:292–323. https://doi.org/10.1016/j.jalz.2016.02.002.

30. Rocchi L, Di Santo A, Brown K, et al. Disentangling EEG responses to TMS due to cortical and peripheral activations. Brain Stimul 2021;14:4–18. https://doi.org/10.1016/j.brs.2020.10.011.

31. Rosanova M, Casali A, Bellina V, et al. Natural frequencies of human corticothalamic circuits. J Neurosci 2009;29:7679–7685. https://doi.org/10.1523/JNEUROSCI.0445-09.2009.

32. Thielscher A, Antunes A, Saturnino GB. Field modeling for transcranial magnetic stimulation: A useful tool to understand the physiological effects of TMS? *2015 37th Annual International Conference of the IEEE Engineering in Medicine and Biology Society (EMBC)*, 2015;222-225. https://doi.org/10.1109/EMBC.2015.7318340.

33. Casula EP, Tieri G, Rocchi L, et al. Feeling of ownership over an embodied avatar's hand brings about fast changes of fronto-parietal cortical dynamics. J Neurosci 2022;42:692–701. https://doi.org/10.1523/JNEUROSCI.0636-21.2021.

34. Casula EP, Pellicciari MC, Picazio S, et al. Spike-timing-dependent plasticity in the human dorso-lateral prefrontal cortex. Neuroimage 2016;143:204–213. https://doi.org/10.1016/j.neuroimage.2016.08.060.

35. Rogasch NC, Fitzgerald PB. Assessing cortical network properties using TMS–EEG. Hum Brain Mapp 2013;34:1652–1669. https://doi.org/10.1002/hbm.22016.

36. Maris E, Oostenveld R. Nonparametric statistical testing of EEG- and MEG-data. J Neurosci Methods 2007;164:177–190. https://doi.org/10.1016/j.jneumeth.2007.03.024.

37. Zott B, Simon MM, Hong W, et al. A vicious cycle of β amyloid–dependent neuronal hyperactivation. Science 2019;365:559–565. https://doi.org/10.1126/science.aay0198.

38. Busche MA, Chen X, Henning HA, et al. Critical role of soluble amyloid-β for early hippocampal hyperactivity in a mouse model of Alzheimer's disease. Proc Natl Acad Sci 2012;109:8740–8745. https://doi.org/10.1073/pnas.1206171109.

39. Mesulam MM, Mufson EJ, Levey AI, Wainer BH. Cholinergic innervation of cortex by the basal forebrain: Cytochemistry and cortical connections of the septal area, diagonal band nuclei, nucleus basalis (Substantia innominata), and hypothalamus in the rhesus monkey. J Comp Neurol 1983;214:170–197. https://doi.org/10.1002/cne.902140206.

40. Machado A, Ferreira D, Grothe MJ, et al. The cholinergic system in subtypes of Alzheimer's disease: an in vivo longitudinal MRI study. Alzheimer's Res Ther 2020;12:51. https://doi.org/10.1186/s13195-020-00620-7.

41. Geula C. Abnormalities of neural circuitry in Alzheimer's disease: hippocampus and cortical cholinergic innervation. Neurology 1998;51:S18–S29. https://doi.org/10.1212/WNL.51.1_Suppl_1.S18.

42. George AA, Vieira JM, Xavier-Jackson C, et al. Implications of oligomeric amyloid-Beta (oAβ42) signaling through α7β2-nicotinic acetylcholine receptors (nAChRs) on basal forebrain cholinergic neuronal intrinsic excitability and cognitive decline. J Neurosci 2021;41:555–575. https://doi.org/10.1523/JNEUROSCI.0876-20.2020.

43. Ikonomovic MD, Klunk WE, Abrahamson EE, et al. Precuneus amyloid burden is associated with reduced cholinergic activity in Alzheimer disease. Neurology 2011;77:39–47. https://doi.org/10.1212/WNL.0b013e3182231419.

44. Niskanen E, Könönen M, Määttä S, et al. New insights into Alzheimer's disease progression: a combined TMS and structural MRI study. PLoS One 2011;6:e26113. https://doi.org/10.1371/journal.pone.0026113.

45. Bonnì S, Veniero D, Mastropasqua C, et al. TMS evidence for a selective role of the precuneus in source memory retrieval. Behav Brain Res 2015;282:70–75.

46. Mancini M, Mastropasqua C, Bonnì S, et al. Theta burst stimulation of the Precuneus modulates resting state connectivity in the left temporal pole. Brain Topogr 2017;30:312–319. https://doi.org/10.1007/s10548-017-0559-x.

47. Koch G, Casula EP, Bonnì S, et al. Precuneus magnetic stimulation for Alzheimer's disease: a randomized, sham-controlled trial. Brain In press.

48. Casula EP, Mayer IMS, Desikan M, et al. Motor cortex synchronization influences the rhythm of motor performance in premanifest huntington's disease. Mov Disord 2018;33:440–448. https://doi.org/10.1002/mds.27285.

49. Palmqvist S, Schöll M, Strandberg O, et al. Earliest accumulation of β-amyloid occurs within the default-mode network and concurrently affects brain connectivity. Nat Commun 2017;8:1214. https://doi.org/10.1038/s41467-017-01150-x.

50. Braak H, Braak E. Neuropathological stageing of Alzheimer-related changes. Acta Neuropathol 1991;82:239–259. https://doi.org/10.1007/BF00308809.

51. Casula EP, Pellicciari MC, Bonnì S, et al. Decreased frontal gamma activity in Alzheimer disease patients. Ann Neurol 2022;92:464–475. https://doi.org/10.1002/ana.26444.

52. Nikulin VV, Kičić D, Kähkönen S, Ilmoniemi RJ. Modulation of electroencephalographic responses to transcranial magnetic stimulation: evidence for changes in cortical excitability related to movement. Eur J Neurosci 2003;18:1206–1212. https://doi.org/10.1046/j.1460-9568.2003.02858.x.

53. Massimini M, Ferrarelli F, Huber R, et al. Breakdown of cortical effective connectivity during sleep. Science 2005;309:2228–2232. https://doi.org/10.1126/science.1117256.

54. Kähkönen S, Komssi S, Wilenius J, Ilmoniemi RJ. Prefrontal transcranial magnetic stimulation produces intensity-dependent EEG responses in humans. Neuroimage 2005;24:955–960. https://doi.org/10.1016/j.neuroimage.2004.09.048.

55. Belardinelli P, König F, Liang C, et al. TMS-EEG signatures of glutamatergic neurotransmission in human cortex. Sci Rep 2021;11:8159. https://doi.org/10.1038/s41598-021-87533-z.

56. Cash RFH, Noda Y, Zomorrodi R, et al. Characterization of glutamatergic and GABAA-mediated neurotransmission in motor and dorsolateral prefrontal cortex using paired-pulse TMS–EEG. Neuropsychopharmacology 2017;42:502–511. https://doi.org/10.1038/npp.2016.133.

57. Noda Y, Zomorrodi R, Cash RFH, et al. Characterization of the influence of age on GABAA and glutamatergic mediated functions in the dorsolateral prefrontal cortex using paired-pulse TMS-EEG. Aging 2017;9:556–567. https://doi.org/10.18632/aging.101178.

58. Barr MS, Farzan F, Davis KD, et al. Measuring GABAergic inhibitory activity with TMS-EEG and its potential clinical application for chronic pain. J Neuroimmune Pharmacol 2013;8:535–546. https://doi.org/10.1007/s11481-012-9383-y.

59. Premoli I, Rivolta D, Espenhahn S, et al. Characterization of GABAB-receptor mediated neurotransmission in the human cortex by paired-pulse TMS–EEG. Neuroimage 2014;103:152–162. https://doi.org/10.1016/j.neuroimage.2014.09.028.

60. Conde V, Tomasevic L, Akopian I, et al. The non-transcranial TMS-evoked potential is an inherent source of ambiguity in TMS-EEG studies. Neuroimage 2019;185:300–312. https://doi.org/10.1016/j.neuroimage.2018.10.052.

61. Ye Q, Zou F, Dayan M, et al. Individual susceptibility to TMS affirms the precuneal role in meta-memory upon recollection. Brain Struct Funct 2019;224:2407–2419. https://doi.org/10.1007/s00429-019-01909-6.

62. Kraft A, Dyrholm M, Kehrer S, et al. TMS over the right precuneus reduces the bilateral field advantage in visual short term memory capacity. Brain Stimul 2015;8:216–223. https://doi.org/10.1016/j.brs.2014.11.004.

63. Hebscher M, Meltzer JA, Gilboa A. A causal role for the precuneus in network-wide theta and gamma oscillatory activity during complex memory retrieval. eLife 2019;8:e43114. https://doi.org/10.7554/eLife.43114.